THE GEOLOGICAL SOCIETY OF AMERICA®

Paleo-Asian oceanic slab under the North China craton revealed by carbonatites derived from subducted limestones

Chunfei Chen[1], Yongsheng Liu[1]*, Stephen F. Foley[2], Mihai N. Ducea[3,4], Detao He[1], Zhaochu Hu[1], Wei Chen[1], and Keqing Zong[1]

[1]State Key Laboratory of Geological Processes and Mineral Resources, School of Earth Sciences, China University of Geosciences, Wuhan 430074, China

[2]ARC Centre of Excellence for Core to Crust Fluid Systems, Department of Earth and Planetary Sciences, Macquarie University, North Ryde, New South Wales 2109, Australia

[3]Department of Geosciences, University of Arizona, Tucson, Arizona 85721, USA

[4]Faculty of Geology and Geophysics, University of Bucharest, Bucharest, Romania

ABSTRACT

It is widely accepted that the lithospheric mantle under the North China craton (NCC) has undergone comprehensive refertilization due to input from surrounding subducted slabs. However, the possible contribution from the Paleo-Asian oceanic slab to the north is poorly constrained, largely because of the lack of convincing evidence for the existence of this slab under the NCC. We report here carbonatite intruding Neogene alkali basalts in the Hannuoba region, close to the northern margin of the NCC. Trace element patterns with positive Sr and U anomalies, negative high field strength elements (Nb, Ta, Zr, Hf, and Ti) and Ce anomalies, high $^{87}Sr/^{86}Sr$ ratios (0.70522–0.70796), and high $\delta^{18}O_{SMOW}$ (standard mean ocean water) values (22.2‰–23‰) indicate that this carbonatite had a limestone precursor. However, the presence of coarse-grained mantle-derived clinopyroxene, orthopyroxene, and olivine, and chemical features of the carbonates suggest that the carbonate melts were derived from the mantle. The carbonates have high $^{143}Nd/^{144}Nd$ ratios (0.51282–0.51298) and show negative correlation between CaO and Ni contents, resulting from reaction between carbonate melt and peridotite. Considering the regional tectonic setting, the carbonatite probably formed by melting of subducted sedimentary carbonate rocks that formed part of the Paleo-Asian oceanic slab, and thus could provide the first direct evidence for the presence of the Paleo-Asian oceanic slab beneath the NCC.

INTRODUCTION

Carbonate platforms are common in oceanic realms. Small tropical oceans, exemplified by many segments of the Tethys Ocean in Europe, were covered with extensive carbonate platforms, found today in classic Alpine fold and thrust belts. It is clear that some of these materials are subducted to mantle depths where they undergo decarbonation reactions and may be involved in partial melting (Collins et al., 2015; Doucelance et al., 2014; Ducea et al., 2005; Hammouda, 2003). Enormous budgets of CO_2 at magmatic arcs (Lee and Lackey, 2015) independently require that carbonate is very influential in mass exchange at convergent margins. Subduction magmatism is probably one of the most important tectonic mechanisms responsible for regulating the exchange of CO_2 between the Earth's interior and the atmosphere (McKenzie et al., 2016). Unfortunately, very few observational data exist to provide details on the mechanisms of transport of carbonate materials and CO_2 from the surface to mantle depths and back to the Earth's surface via fluid (decarbonation reactions) and melt transport (Liu et al., 2015).

It has been suggested that the lithosphere of the North China craton (NCC) was successively modified by (1) the southward subduction of the Paleo-Asian oceanic slab (PAOS) between the early Paleozoic and the late Permian, (2) the northward subduction of the Paleo-Tethys oceanic and Yangtze plates in the Triassic, and (3) the westward subduction of the Pacific plate since the Cretaceous (Fig. 1A) (Windley et al., 2010). Although all of these subduction events could have contributed to widespread lithospheric reactivation and thinning under the NCC (e.g., Griffin et al., 1998), the Pacific plate subduction was generally advocated to account for the lithospheric thinning (Zhu et al., 2011). The contribution of the PAOS and Paleo-Tethys oceanic slab to lithospheric thinning remains enigmatic, largely because of the lack of convincing evidence for the existence of these slabs under the NCC. If abundant carbonate sediments were transported into deep mantle during oceanic slab subduction, they could have contributed fundamentally to the modification of the chemical and physical properties of the lithospheric mantle by carbonate metasomatism. In turn, subsequent mantle-derived melts (especially carbonatite) could contain the fingerprint of subducted carbonate, which can be used to trace the origin of the subducted slab (Tappert et al., 2009) and outline the crust-mantle recycling of carbonate sediments.

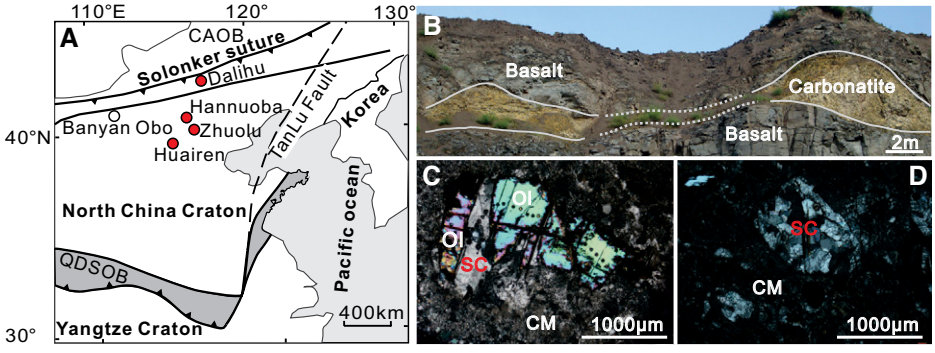

Figure 1. A: Tectonic framework of the study area (modified from Windley et al., 2010). CAOB—Central Asian orogenic belt; QDSOB—Qinling-Dabie-Sulu orogenic belt. B: Field appearance of the carbonatite intrusion. C: Residual olivine (Ol) xenocryst partly resorbed by carbonatite melt. SC—sparry calcite; CM—carbonate matrix. D: Monomineralic aggregates consist of interlocking calcite grains.

*E-mail: yshliu@hotmail.com

Data Repository item 2016347 | doi:10.1130/G38365.1

Here we document a carbonatite intrusion with geochemical features of recycled limestone. The intrusion marks the subduction of an overlying carbonate platform of the PAOS, to mantle depths beneath the NCC, providing evidence for recycling of carbonate back to the Earth's surface by buoyant diapirism and high-degree melting.

SAMPLES, PETROLOGY, AND GEOCHEMICAL COMPOSITIONS

Samples were collected from a carbonatite intrusion (0.5–3 m thick and >35 m wide) that intrudes Neogene basalts (22–10 Ma; Zhu, 1998) at Hannuoba (eastern China; Fig. 1). The basalts are distributed along the northern margin of the NCC, and comprise intercalated tholeiitic, transitional, and alkali basalts (Zhi et al., 1990). The source of the basalts probably contains abundant garnet-pyroxenite (Liu et al., 2008) or was metasomatized by carbonate-rich fluid (Dupuy et al., 1992). The alkali basalts carry abundant granulite, pyroxenite, and peridotite xenoliths (Chen et al., 2001). The evolved Sr-Nd isotopic compositions of some pyroxenite xenoliths indicate involvement of subducted sediments (e.g., Xu, 2002). The carbonatite intrusion occurs in xenolith-free basalt and has a sharp boundary with the basalt layer. The overlying basalt is domed upward by the invasion of the carbonatite melt (Fig. 1B).

The carbonatite contains aggregates of calcite phenocrysts and medium- to coarse-grained silicate macrocrysts set in a matrix of fine-grained calcite (Figs. 1C and 1D), indicating rapid quenching. Monomineralic aggregates of interlocking calcite grains (50–100 μm) indicate calcite accumulation before quenching. The silicate macrocrysts consist of coarse-grained clinopyroxene (Cpx, 0–15 vol%), orthopyroxene (Opx, 0–12 vol%), olivine (Ol, 0–10 vol%), and rare spinel (Sp, 0–1.5 vol%). Ol is forsteritic ($Fo_{90–91}$) and has low CaO contents (<0.1 wt%) but high Ni contents (2809–3062 ppm), and Opx and Cpx have Mg# values of 90.8–91.6 and 91.9–93.3, respectively (Table DR1 in the GSA Data Repository[1]). Many macrocrysts consist of recrystallized pseudomorphs of calcite replacing the silicate minerals, indicating resorption in the carbonate melt (Fig. 1C). Moissanite (20–80 μm), highly disordered graphite (10–30 μm), and Na-K chlorides (~20 μm) were found (Fig. DR1). Moissanite was identified by characteristic Raman peaks at 769, 791, and 970 cm^{-1} and highly disordered graphite was identified by Raman bands at 1358 cm^{-1} and 1589 cm^{-1} (Fig. DR1).

Whole-rock compositions of the carbonatites have high CaO (44.1–53.9 wt%), intermediate MgO (0.8–4.8 wt%), and low alkali contents (Na_2O <0.01 wt% and K_2O <0.05 wt%); many are similar to limestones, and some are along a mixing trend between limestone and peridotite (Fig. DR2). MgO contents in the carbonatites are higher than in limestones (0.13–1.65 wt%), and show a negative correlation with CaO. Trace element patterns are similar to sedimentary limestones with notably positive Sr and U anomalies and negative high field strength element (HFSE; Zr, Hf, Nb, Ta, Ti) anomalies (Fig. 2). The incompatible trace element contents of most samples are lower than average limestone, especially for Rb, Ba, and heavy rare earth elements (REEs) (Fig. 2). Their REE patterns show negative Ce anomalies (Ce/Ce* = 0.2–0.8) and positive Eu anomalies (Eu/Eu* = 1.15–2.98) (Table DR2). The carbonate matrix contains 45.2–52.7 wt% CaO, 0.4–1.8 wt% MgO, and 1.5–5.0 wt% SiO_2 (Table DR3). Both the carbonate matrix and phenocrysts have higher Ni contents (1–133 ppm) than limestone, and show negative correlations between CaO and Ni (Fig. 3A).

Carbonates in the carbonatite intrusion have higher $^{87}Sr/^{86}Sr$ (0.70522–0.70796) and slightly higher $^{143}Nd/^{144}Nd$ (0.51282–0.51298) than typical carbonatites (Fig. 3B). $^{143}Nd/^{144}Nd$ ratios show no correlation with Nd contents (0.4–2.8 ppm), whereas $^{87}Sr/^{86}Sr$ ratios correlate negatively with Sr contents (27–306 ppm) (Fig. DR3). Rare aragonite veinlets that crosscut one sample have high Sr contents (2507–6600 ppm) and relatively low $^{87}Sr/^{86}Sr$ ratios (0.70411–0.70683) (Table DR4); the postmagmatic fluid that deposited this aragonite might have also partially modified the sample (Fig. 3B). The primary carbonatitic melts represented by the low-Sr samples have the highest $^{87}Sr/^{86}Sr$ and $^{143}Nd/^{144}Nd$ ratios. The carbonatites are characterized by light carbon isotopic compositions [$\delta^{13}C_{VPDB}$ (Vienna Peedee belemnite) = −14.4‰ to −11.2‰] but heavy oxygen isotopic compositions [$\delta^{18}O_{SMOW}$ (SMOW—standard mean ocean water) = 22.2‰ to 23‰] (Table DR2).

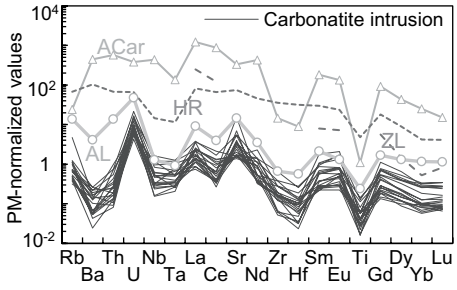

Figure 2. Primitive mantle (PM) normalized trace element patterns for Hannuoba carbonatite intrusion compared to average carbonatite (ACarb) and average limestone (AL) (data sources are provided in the Data Repository [see footnote 1]). The Mesozoic Zhuolu (ZL) and Huairen (HR) carbonatite data are from Yan et al. (2007), and primitive mantle values are from McDonough and Sun (1995).

DISCUSSION

Mantle Derivation of the Carbonatite

Possible origins of the Ol and Cpx macrocrysts in the carbonatite intrusion are reaction products between carbonate melt and the basalt wall rock (Jolis et al., 2013) or peridotite xenocrysts from the mantle that potentially provide records of the ascent process of the carbonatite melts. The compositions of Ol (CaO <0.1 wt%) and Cpx (Mg# = 91.9–93.3 and SiO_2 >50.1 wt%) macrocrysts clearly correspond to minerals in mantle peridotites and are unlike products

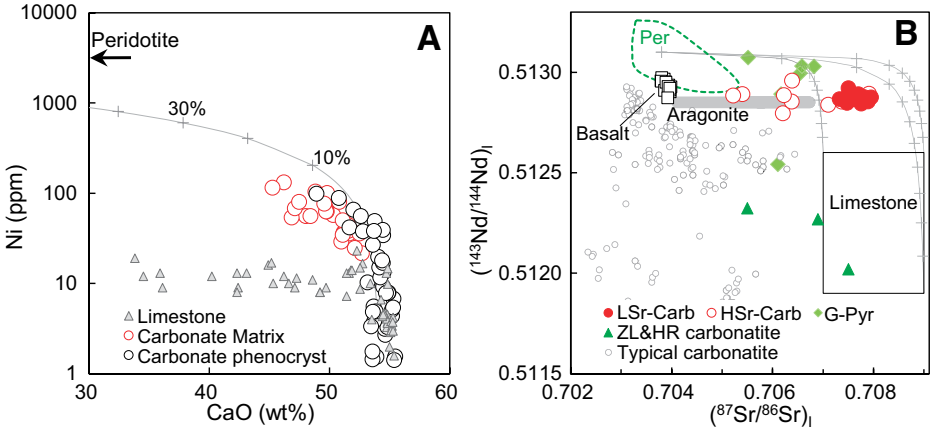

Figure 3. A: Carbonates in the carbonatite intrusion are on a trend between pure calcite and peridotite, in contrast to limestones, which vary in CaO at constantly low Ni. B: Plot of $(^{87}Sr/^{86}Sr)_I$-$(^{143}Nd/^{144}Nd)_I$. The age of the carbonatite intrusion was assumed to be the same as the Hannuoba basalt (22 Ma). $^{143}Nd/^{144}Nd$ ratios of aragonite veinlets (gray bar) are represented by the intrusion. Solid curves are mixing lines between limestone and Hannuoba peridotite (Per); ticks on curves show 10% increments. HSr-Carb—carbonatite with Sr >60 ppm, LSr-Carb—carbonatite with Sr <60 ppm; G-Pyr—Hannuoba garnet pyroxenite; Basalt—Hannuoba alkali basalts; ZL— Zhuolu; HR—Huairen. See the Data Repository (see footnote 1) for detailed explanation, data sources, and modeling parameters.

[1]GSA Data Repository item 2016347, description of analytical methods, Figures DR1–DR5, and Tables DR1–DR4, is available online at http://www.geosociety.org/pubs/ft2016.htm or on request from editing@geosociety.org.

of carbonate melt–basalt interaction (Fig. DR4). This conclusion is supported by the Ni contents of Opx and Cpx (Table DR1), which are also typical for mantle minerals (Foley et al., 2006). Ol produced by carbonate melt–basalt interaction would have higher CaO (>1.31 wt%), and Cpx would be characterized by low Mg# (<84) and low SiO_2 content (<45 wt%) (Jolis et al., 2013). The temperatures estimated from Cpx + Opx macrocryst pairs are 770–932 °C (see the Data Repository), implying a source depth of ~50 km for the disrupted mantle xenoliths on the documented geotherm for the northern margin of the NCC (Chen et al., 2001). Hydrous carbonatitic liquids are known to occur at temperatures as low as 870–900 °C (Poli, 2015), at the upper end of this temperature range. Furthermore, highly disordered graphite found in the Hannuoba carbonatite intrusion might be the result of the transformation of diamond during rapid upward migration from the deeper mantle, as suggested by diamond-bearing carbonatite xenoliths (Liu et al., 2015). High Ni contents and high $^{143}Nd/^{144}Nd$ ratios of carbonate components in the carbonatite intrusion indicate that interaction between the carbonate melt and peridotite occurred (Fig. 3), as is also demonstrated by resorption of Ol macrocrysts in the carbonatite melt (Fig. 1C). In combination, these observations indicate that the carbonatite melt originated at mantle depths, or at least resided long enough in the mantle to acquire these compositional characteristics.

Subducted Sedimentary Carbonate Precursor for the Carbonatite

Mantle-derived carbonatites typically exhibit enriched incompatible trace element contents [e.g., light (L) REEs, Nb, Sr, and Ba] and steep LREE-enriched patterns (Jones et al., 2013). Contrasting with this, the Hannuoba carbonatites have much lower trace element contents, and show trace element patterns similar to that of limestone (Fig. 2). Furthermore, they have high $\delta^{18}O_{SMOW}$ values (22.2‰–23‰), high $^{87}Sr/^{86}Sr$ ratios (0.70522–0.70796) (Fig. 3B), trace element patterns with positive Sr and U anomalies and negative HFSE and Ce anomalies (Fig. 2), all of which are typical features of sedimentary limestones (Jin et al., 2009). In the CaO-MgO-SiO_2 plot, they form a trend consistent with interaction between pure limestone and peridotite (Fig. DR2); their $^{87}Sr/^{86}Sr$ and $^{143}Nd/^{144}Nd$ ratios and high Ni contents can be modeled by simple mixing between limestone and peridotite (Fig. 3). Taken together, these features suggest that the carbonatite intrusion formed from melts of subducted limestone that interacted with peridotite at depths of at least 50 km and possibly 150 km, incorporating peridotite minerals as xenocrysts.

The incompatible trace elements, especially those highly mobilized in aqueous fluids (e.g., Rb and Ba), have lower concentrations in the Hannuoba carbonatites than in average limestone (Fig. 2), indicating that the subducted limestone precursor could have been partially modified by aqueous fluids in the subduction zone. Furthermore, the much lower heavy (H) REE contents and positive Eu anomalies in the carbonatites compared to average limestone (Fig. 2) might be attributed to modification by subduction-related CO_3^{2-}-rich aqueous fluids. $HREE^{3+}$ are complexed more strongly by CO_3^{2-} than $LREE^{3+}$, and similarly $LREE^{3+}$ are complexed more strongly by CO_3^{2-} than Eu^{2+} (Bau, 1991), so that $HREE^{3+}$ would be removed easily from limestone by a CO_3^{2-}-rich fluid, but Eu^{2+} could be retained.

Melting of limestone is commonly regarded to be restricted to unusually hot regimes (Wyllie and Tuttle, 1960), although the temperatures involved may be reduced in water-bearing conditions (Poli, 2015). Due to the high solidus temperatures but lower density and viscosity, limestone cannot be melted at the top of the subducted slab, but may penetrate the cold cratonic mantle in the form of solid buoyant diapirs (Behn et al., 2011). The large scale of basalts in the Hannuoba area (~1700 km^2) indicates a giant Cenozoic thermal event in the mantle under the northern margin of the NCC that could have resulted in substantial melting of such limestone diapirs. Limestone is mostly composed of a single calcite phase, so it is reasonable to speculate that high modes of melting of subducted limestone would occur once melting initiates. High-degree melting of a subducted limestone in the mantle was also suggested (in Liu et al., 2015) to account for the mantle-derived carbonatite xenoliths from the Dalihu area with the geochemical features of limestone. The Hannuoba carbonatite intrusion may share an origin similar to that of the carbonatite xenoliths reported in Liu et al. (2015), but the intrusion was emplaced into the shallow crust. The carbonatite melt might have undergone complex devolatilization during ascent (Russell et al., 2012), which could have produced the low $\delta^{13}C_{VPDB}$ values of carbonatite melt (Cartigny et al., 1998) and also yielded extremely local, strongly reducing conditions that permitted the formation of moissanite (Shiryaev and Gaillard, 2014). This would explain both the much lower $\delta^{13}C_{VPDB}$ values of the Hannuoba carbonatites relative to average limestone (–0.44‰ ± 2‰; 1σ, n = 102), and the occurrence of moissanites in the Hannuoba intrusion (Fig. DR1).

Implications for the Subduction of the Paleo-Asian Oceanic Slab Under the NCC

The $^{87}Sr/^{86}Sr$ ratios of sedimentary carbonate rocks have varied with time (Veizer et al., 1999) (Fig. DR5), so that the high Sr isotopic compositions can be used to constrain the age of the limestone. $^{87}Sr/^{86}Sr$ ratios of marine carbonates increased from ≤0.702 in the Archean to ~0.7069 in the late Neoproterozoic, and varied within a small range (0.7069–0.7089) during the Phanerozoic. The highest $^{87}Sr/^{86}Sr$ ratio (0.70791) of carbonate in the Hannuoba carbonatite represents materials least contaminated by aragonite veins and mantle materials (Fig. 3B), from which we infer that the age of the limestone source of the carbonatite is most probably between 580 and 360 Ma, and certainly not older than 580 Ma (Fig. DR5); this is consistent with its derivation from the Paleo-Asian Ocean, which existed between 1 Ga and 250 Ma (Xiao et al., 2003). Furthermore, the carbonatite intrusion occurs >1000 km from the trench position of the east Pacific plate and the Qinling-Dabie-Sulu orogenic belt, but within 200 km of the northern margin of the NCC (Fig. 1A). The Pacific slab is eliminated as a possible source because it is stagnating in the mantle transition zone beneath the eastern NCC (Zhao et al., 2009) at a depth to which limestone could not be subducted due to its low density and viscosity. These observations suggest that the limestone precursor was most probably derived from the subducted PAOS.

It is noteworthy that Mesozoic carbonatites from Zhuolu and Huairen ~50–100 km south of Hannuoba have high $^{87}Sr/^{86}Sr$ ratios (0.7055–0.7075; Yan et al., 2007) (Figs. 1 and 3B) similar to those of the Hannuoba carbonatite intrusion, implying that they may also be related to the PAOS. Although the Mesozoic Zhuolu and Huairen carbonatites have similarly lower trace element contents than typical carbonatite, they have much higher trace element contents than the Cenozoic Hannuoba intrusion (Fig. 2). This suggests that the Mesozoic carbonatites could have been derived from partial melting of subducted carbonate-rich eclogite rather than limestone. The Hannuoba, Zhuolu, and Huairen carbonatites are distributed in a north-south direction, and show increasing trace element contents with increasing distance from the north margin of the NCC (Figs. 2 and 4). The temporal and spatial variations of the Mesozoic and Cenozoic carbonatites are consistent with the interpretation that carbonated eclogite could have been subducted deep into the mantle (Hammouda, 2003) before melting, whereas limestone would have detached

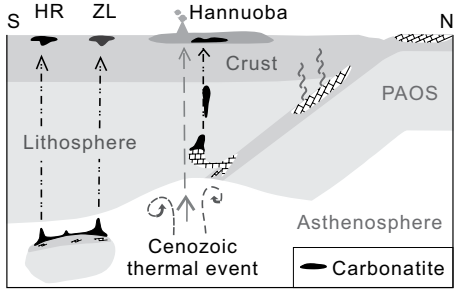

Figure 4. Illustration of recycling of sedimentary limestone caused by subduction of the Paleo-Asian oceanic slab. PAOS—Paleo-Asian oceanic slab; HR—Huairen; ZL— Zhuolu.

from the downgoing slab to form buoyant diapirs penetrating the shallow and cold mantle (Behn et al., 2011; Liu et al., 2015) (Fig. 4). Subsequently, a giant Cenozoic mantle thermal event, as indicated by the large-scale Hannuoba basalts, triggered high-degree melting of the limestones, now in the shallower mantle. These carbonatites reconstruct the path of the consumed PAOS under the NCC, which is critical for understanding how subduction zones modulate the global carbon cycle.

ACKNOWLEDGMENTS

We thank Jussi S. Heinonen, Hugh Smithies, and two anonymous reviewers for helpful reviews that improved the manuscript. This research is cosupported by the National Science Foundation of China (grants 41530211, 41125013, and 90914007), the 973 Project of the Ministry of Science and Technology of China (2013CB429806), the State Administration of Foreign Expert Affairs of China (B07039), the Specialized Research Fund for the Doctoral Program of Higher Education (20130145110001), and Ministry of Science and Technology Special Funds of the State Key Laboratory of Geological Processes and Mineral Resources (China University of Geosciences). This is contribution 852 of the Australian Research Council Centre of Excellence for Core to Crust Fluid Systems, and contribution 1110 of the Geochemical Evolution and Metallogeny of Continents Key Centre (Macquarie University, Australia).

REFERENCES CITED

Bau, M., 1991, Rare-earth element mobility during hydrothermal and metamorphic fluid-rock interaction and the significance of the oxidation state of europium: Chemical Geology, v. 93, p. 219–230, doi:10.1016/0009-2541(91)90115-8.

Behn, M.D., Kelemen, P.B., Hirth, G., Hacker, B.R., and Massonne, H.-J., 2011, Diapirs as the source of the sediment signature in arc lavas: Nature Geoscience, v. 4, p. 641–646, doi:10.1038/ngeo1214.

Cartigny, P., Harris, J.W., and Javoy, M., 1998, Eclogitic diamond formation at Jwaneng: No room for a recycled component: Science, v. 280, p. 1421–1424, doi:10.1126/science.280.5368.1421.

Chen, S.H., O'Reilly, S.Y., Zhou, X.H., Griffin, W.L., Zhang, G.H., Sun, M., Feng, J.L., and Zhang, M., 2001, Thermal and petrological structure of the lithosphere beneath Hannuoba, Sino-Korean Craton, China: Evidence from xenoliths: Lithos, v. 56, p. 267–301, doi:10.1016/S0024-4937(00)00065-7.

Collins, N.C., Bebout, G.E., Angiboust, S., Agard, P., Scambelluri, M., Crispini, L., and John, T., 2015, Subduction zone metamorphic pathway for deep carbon cycling: II. Evidence from HP/UHP metabasaltic rocks and ophicarbonates: Chemical Geology, v. 412, p. 132–150, doi:10.1016/j.chemgeo.2015.06.012.

Doucelance, R., Bellot, N., Boyet, M., Hammouda, T., and Bosq, C., 2014, What coupled cerium and neodymium isotopes tell us about the deep source of oceanic carbonatites: Earth and Planetary Science Letters, v. 407, p. 175–186, doi:10.1016/j.epsl.2014.09.042.

Ducea, M.N., Saleeby, J., Morrison, J., and Valencia, V.A., 2005, Subducted carbonates, metasomatism of mantle wedges, and possible connections to diamond formation: An example from California: American Mineralogist, v. 90, p. 864–870, doi:10.2138/am.2005.1670.

Dupuy, C., Liotard, J., and Dostal, J., 1992, Zr/Hf fractionation in intraplate basaltic rocks: Carbonate metasomatism in the mantle source: Geochimica et Cosmochimica Acta, v. 56, p. 2417–2423, doi:10.1016/0016-7037(92)90198-R.

Foley, S.F., Andronikov, A.V., Jacob, D.E., and Melzer, S., 2006, Evidence from Antarctic mantle peridotite xenoliths for changes in mineralogy, geochemistry and geothermal gradients beneath a developing rift: Geochimica et Cosmochimica Acta, v. 70, p. 3096–3120, doi:10.1016/j.gca.2006.03.010.

Griffin, W.L., Andi, Z., O'Reilly, S.Y., and Ryan, C.G., 1998, Phanerozoic evolution of the lithosphere beneath the Sino-Korean craton, *in* Flower, M.F.J., et al., eds., Mantle dynamics and plate interactions in East Asia: American Geophysical Union Geodynamics Series Volume 27, p. 107–126, doi:10.1029/GD027p0107.

Hammouda, T., 2003, High-pressure melting of carbonated eclogite and experimental constraints on carbon recycling and storage in the mantle: Earth and Planetary Science Letters, v. 214, p. 357–368, doi:10.1016/S0012-821X(03)00361-3.

Jin, Z.J., Zhu, D.Y., Hu, W.X., Zhang, X.F., Zhang, J.T., and Song, Y.C., 2009, Mesogenetic dissolution of the middle Ordovician limestone in the Tahe oilfield of Tarim basin, NW China: Marine and Petroleum Geology, v. 26, p. 753–763, doi:10.1016/j.marpetgeo.2008.08.005.

Jolis, E.M., Freda, C., Troll, V.R., Deegan, F.M., Blythe, L.S., McLeod, C.L., and Davidson, J.P., 2013, Experimental simulation of magma-carbonate interaction beneath Mt. Vesuvius, Italy: Contributions to Mineralogy and Petrology, v. 166, p. 1335–1353, doi:10.1007/s00410-013-0931-0.

Jones, A.P., Genge, M., and Carmody, L., 2013, Carbonate melts and carbonatites: Reviews in Mineralogy and Geochemistry, v. 75, p. 289–322, doi:10.2138/rmg.2013.75.10.

Lee, C.-T.A., and Lackey, J.S., 2015, Global continental arc flare-ups and their relation to long-term greenhouse conditions: Elements, v. 11, p. 125–130, doi:10.2113/gselements.11.2.125.

Liu, Y.S., Gao, S., Kelemen, P.B., and Xu, W.L., 2008, Recycled crust controls contrasting source compositions of Mesozoic and Cenozoic basalts in the North China Craton: Geochimica et Cosmochimica Acta, v. 72, p. 2349–2376, doi:10.1016/j.gca.2008.02.018.

Liu, Y.S., He, D.T., Gao, C.G., Foley, S.F., Gao, S., Hu, Z.C., Zong, K.Q., and Chen, H.H., 2015, First direct evidence of sedimentary carbonate recycling in subduction-related xenoliths: Scientific Reports, v. 5, p. 11547, doi:10.1038/srep11547.

McDonough, W.F., and Sun, S.S., 1995, The composition of the Earth: Chemical Geology, v. 120, p. 223–253, doi:10.1016/0009-2541(94)00140-4.

McKenzie, N.R., Horton, B.K., Loomis, S.E., Stockli, D.F., Planavsky, N.J., and Lee, C.-T.A., 2016, Continental arc volcanism as the principal driver of icehouse-greenhouse variability: Science, v. 352, p. 444–447, doi:10.1126/science.aad5787.

Poli, S., 2015, Carbon mobilized at shallow depths in subduction zones by carbonatitic liquids: Nature Geoscience, v. 8, p. 633–636, doi:10.1038/ngeo2464.

Russell, J.K., Porritt, L.A., Lavallee, Y., and Dingwell, D.B., 2012, Kimberlite ascent by assimilation-fuelled buoyancy: Nature, v. 481, p. 352–356, doi:10.1038/nature10740.

Shiryaev, A.A., and Gaillard, F., 2014, Local redox buffering by carbon at low pressures and the formation of moissanite–natural SiC: European Journal of Mineralogy, v. 26, p. 53–59, doi:10.1127/0935-1221/2013/0025-2339.

Tappert, R., Foden, J., Stachel, T., Muehlenbachs, K., Tappert, M., and Wills, K., 2009, Deep mantle diamonds from South Australia: A record of Pacific subduction at the Gondwanan margin: Geology, v. 37, p. 43–46, doi:10.1130/G25055A.1.

Veizer, J., et al., 1999, $^{87}Sr/^{86}Sr$, $\delta^{13}C$ and $\delta^{18}O$ evolution of Phanerozoic seawater: Chemical Geology, v. 161, p. 59–88, doi:10.1016/S0009-2541(99)00081-9.

Windley, B.F., Maruyama, S., and Xiao, W.J., 2010, Delamination/thinning of sub-continental lithospheric mantle under eastern China: The role of water and multiple subduction: American Journal of Science, v. 310, p. 1250–1293, doi:10.2475/10.2010.03.

Wyllie, P.J., and Tuttle, O.F., 1960, The system CaO-CO_2-H_2O and the origin of carbonatites: Journal of Petrology, v. 1, p. 1–46, doi:10.1093/petrology/1.1.1.

Xiao, W.J., Windley, B.F., Hao, J., and Zhai, M.G., 2003, Accretion leading to collision and the Permian Solonker suture, Inner Mongolia, China: Termination of the central Asian orogenic belt: Tectonics, v. 22, 1069, doi:10.1029/2002TC001484.

Xu, Y.G., 2002, Evidence for crustal components in the mantle and constraints on crustal recycling mechanisms: Pyroxenite xenoliths from Hannuoba, north China: Chemical Geology, v. 182, p. 301–322, doi:10.1016/S0009-2541(01)00300-X.

Yan, G.H., Mu, B.L., Zeng, Y.S., Cai, J.H., Ren, K.X., and Li, F.T., 2007, Igneous carbonatites in North China craton: The temporal and spatial distribution, Sr and Nd isotopic characteristics and their geological significance: Geological Journal of China Universities, v. 13, p. 463–473 (in Chinese with English abstract).

Zhao, D.P., Tian, Y., Lei, J.S., Liu, L., and Zheng, S.H., 2009, Seismic image and origin of the Changbai intraplate volcano in East Asia: Role of big mantle wedge above the stagnant Pacific slab: Physics of the Earth and Planetary Interiors, v. 173, p. 197–206, doi:10.1016/j.pepi.2008.11.009.

Zhi, X.C., Song, Y., Frey, F.A., Feng, J.L., and Zhai, M.Z., 1990, Geochemistry of Hannuoba basalts, eastern China: Constraints on the origin of continental alkalic and tholeiitic basalt: Chemical Geology, v. 88, p. 1–33, doi:10.1016/0009-2541(90)90101-C.

Zhu, B.Q., 1998, Theory and applications of isotope systematics in geosciences: Evolution of continental crust and mantle in China: Beijing, Science Press, 330 p.

Zhu, R.X., Chen, L., Wu, F.Y., and Liu, J.L., 2011, Timing, scale and mechanism of the destruction of the North China Craton: Science China Earth Sciences, v. 54, p. 789–797, doi:10.1007/s11430-011-4203-4.

Manuscript received 15 July 2016
Revised manuscript received 27 September 2016
Manuscript accepted 29 September 2016

Printed in USA